



1 *Conference Proceedings Paper*

2 **Determination of Alteration Zones Using** 3 **Hyperspectral Imagery Based on Spectral Unmixing**

4 **Seyd Teymoor Seydi^{1,*}, Mohammad Reza Yousefi²**

5 ¹ School of Surveying and Geospatial Engineering, College of Engineering, University of Tehran, Tehran,
6 Iran; seydi.teymoor@ut.ac.ir

7 ² Institute of geophysics, University of Tehran, Tehran, Iran; mr.yosefi@ut.ac.ir

8 * Correspondence: Seydi.teymoor@ut.ac.ir; Tel.: +98 939-263-3659

9 **Abstract:** The remote sensing as a new technology provides data from earth with lowest cost and
10 time. The Central Iranian Volcanic Belt is a volcano-plutonic complex which contains extrusive and
11 intrusive rocks of Eocene to Quaternary age. In this area, the Meyduk porphyry copper deposit (55°
12 10' 05" E, 30° 25' 10" N) is located 45 km northeast of Shahr-e Babak city. The Cu-mineralization and
13 associated hydrothermal alteration zones are focused on the Miocene dioritic and Eocene andesitic
14 rocks. Today, remote sensing with having high spatial and spectral resolution, wide coverage and
15 the lowest cost plays a key role in the field of earth sciences research (especially in the mineral ore
16 explorations). In this case, hyperspectral images have a special status in remote sensing. Even
17 though these images have a high spectral resolution, they have not a high spatial resolution. Because
18 of the presence of different prospectives on a ground pixel, the amount of received energy by the
19 receiver is the combination of multiple ground effects. Therefore, low spatial resolution of
20 hyperspectral images can be a reason for spectral mixing in these images. The purpose of spectral
21 separation is recognition of observed surface components and calculation of abundance of the inside
22 component of each pixel area. The purpose of applying unmixing algorithm is estimation and
23 extraction of presence percentage of any considered mineral ores in each pixel of the image. We
24 applied mentioned algorithm in three steps. In the first one, estimation of a number of the mineral
25 ore types using Hysime algorithm is done. In the next step, we extracted spectral signature of each
26 of these mineral ores using N-finder and in the final step, we calculated vector abundance of them
27 using FLS algorithm.

28 **Keywords:** mineral alterations, remote sensing, hyperspectral, unmixing, mineral map.
29

30 **1. Introduction**

31 Remote sensing (RS) is kind of new source of numerous applications in the field of Earth Sciences
32 that studies one of the most important applications identified changes to the Earth's surface[1].
33 Today, remote sensing with having high spatial and spectral resolution, wide coverage and the
34 lowest cost plays a key role in the field of earth sciences research and has many application[2]. These
35 applications are: mineral mapping, disaster monitoring, urban monitoring, and wetland
36 monitoring[3].

37 Recently, to development hyperspectral sensors and improvement of quality data, the using of
38 hyperspectral dataset covert to hot subject between researchers. This theme can be seen in many
39 applications such as: classification, anomaly detection, change detection and mineral mapping[4-7].
40 Most hyperspectral imagery has high spectral resolution with low spatial resolution [8,9]. Also, the
41 complex diversity of scene caused the spectrum gained in one pixel of a hyperspectral image may
42 mix with some material [8,9]. The spectral unmixing is a processing that decomposing each mixed

43 pixel into a set of abundances pure endmembers. The unmixing provides details information on each
44 pixel in the hyperspectral image in terms of abundance.

45 **2. Proposed Method**

46 2.1 Unmixing

47 The spectral Unmixing was applied in three steps: 1) Estimation of endmembers using Hysime
48 algorithm, 2) Extraction of enmembers using Sisal and N-finder algorithms and 3) Calculation of
49 vector abundance using fully least square error (FLS) algorithm. We explain the details of algorithm
50 at next steps.

51 2.1.1. Endmember Estimation

52 The endmember estimation is first step for unmixing that applied by many algorithms. We used
53 Hysime endmember estimation due to it is simple and common in spectral unmixing Hyperspectral
54 imagery field. The main basic idea Hysime algorithm is use of correlation and noise matrix for
55 estimation of endmember[10].

56 The purpose of this section is estimation of endmembers that is carried out using Hysime
57 algorithm. This algorithm is one of the automatically intrinsic dimension estimation methods. This
58 method starts with estimation of noise correlation matrix and signal matrix. Then a subset of Eigen
59 vector values (corresponding to the number of endmembers) is selected so that it can represent the
60 subspace under the least error[10].

61 2.1.2. Endmember Extraction

62 Extraction of endmembers using Sisal and N-finder algorithms were done. These algorithms are
63 widely used in remote sensing. The main idea of the mentioned algorithms is to find pixels that can
64 make maximum simplex volume.

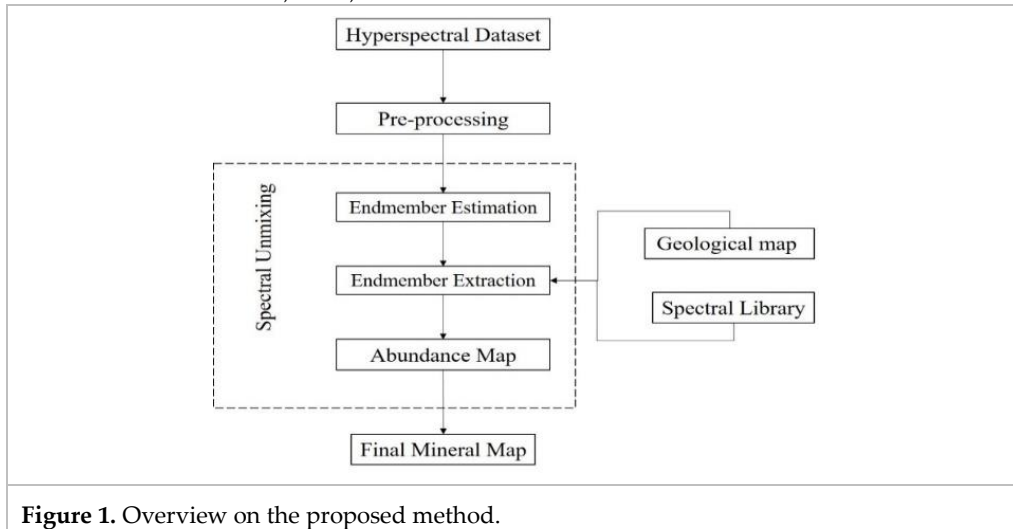
65 These pixels are considered as endmembers. Due to complex mathematics of finding
66 endmembers, this only be considered as an optimal estimate of the problem[11].

67 2.1.3. Abundance Map

68 The abundance of each extracted end member will be calculated using the fully least squares
69 error algorithm for each pixel of the predictor phase. The main idea of this algorithm is to find the
70 abundance of one of each endmember, so that the amount of positive and total abundance of each
71 endmember from each pixel is equal to one. Each pixel is decided thorough calculating the
72 abundance[12].

73 2.2. Proposed Framework

74 We extracted endmembers from hyperspectral dataset using spectral unmixing and assigned
75 them to one of the mineral objects. For this purpose, we used spectral library and geological map, so
76 that attributed the spectral signatures that have more similarity to which mineral objects in spectral
77 library. It's noticeable to say, we used the geological map for areas where we have more than one
78 spectral signature. The figure 1 presents proposed method flowchart.



79 **3. Geology of the area**

80 Meyduk (Latala) area is located in Shahre Babak (Kerman province). The rock outcrops of
 81 Meyduk exploratory (Latala) area is included a small part of the northeastern border of Shahre Babak
 82 sheet. The most significant feature of the mineralization in the study area is vein-veinlet
 83 mineralization zones which are controlled by faults and fault zones[13].

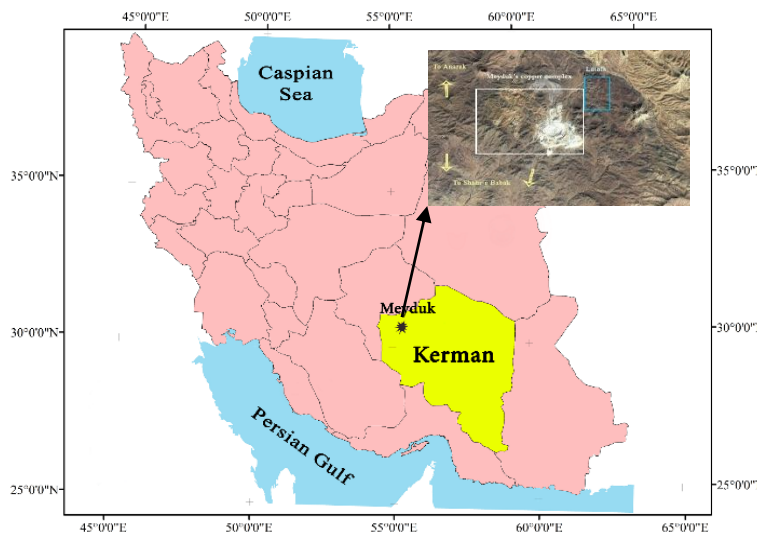


Figure 2. The location of Meyduk in Kerman province and satellite image of the area that indicates relative position of Latala.

84 **3.1 Mineralization**

85 As we mentioned, the most important feature of the mineralization in the study area is vein-
 86 veinlet mineralization zones which are controlled by faults and fault zones. In total seven veins were
 87 detected which are along the mostly north-south to NW-SE (Figure 3-a). Width of the mineralized
 88 veins are from 20 cm to 20 m and they visible up to 1300 meters. The main mineralized veins contain
 89 quartz, goethite, hematite, calcite, clay minerals and calcite.

90 The figure 3-b presents false colour composite of the area.

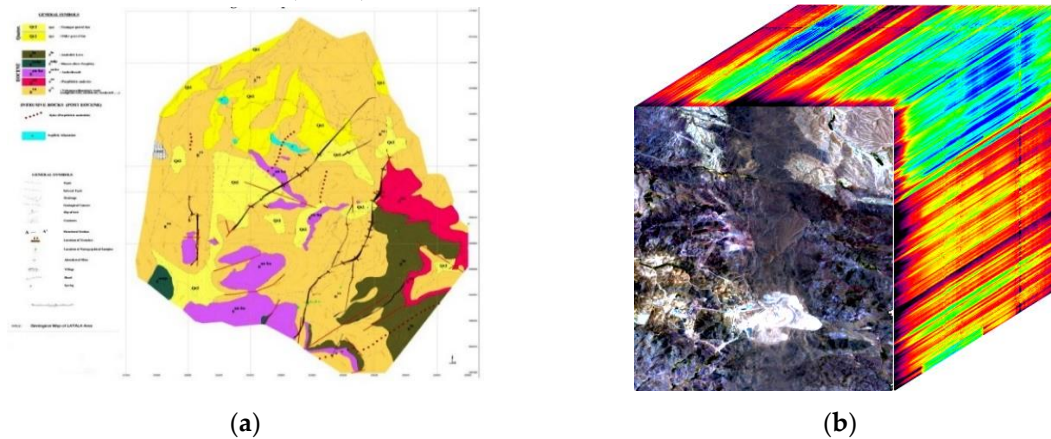


Figure 3. (a) geological map of the area, and (b) showing false color composition that is derived from hyperspectral data in Meyduk (Latala) area at 2004.

91 **3.2. Hyperspectral Dataset**

92 In order to evolution of proposed method performance, the real hyperspectral dataset were used
 93 in this research that are related to Hyperion sensors. The Hyperion sensors carried by EO-1 satellite
 94 that it is first spaceborne hyperspectral instrument to acquire data in a wide of spectral bands. The
 95 characteristics of Hyperion dataset sensors has presented in table 1.

Table 1. The characteristics of hyperspectral dataset.

Parameters	Description
Spatial Resolution	30 m
Spectral Resolution	10 nm
Radiometric Resolution	16
Date Acquired	2006
Spectral bands	166

96 **4. Implementation**

97 **4.1. Preprocessing**

98 Due to environmental and equipment conditions, these images have to be applied
 99 preprocessing. The preprocessing are made in two steps: 1) geometric preprocessing and 2) spectral
 100 preprocessing[14].

101 The spectral preprocessing contains: 1) remove no-data bands, 2) spatial shift correction for
 102 SWIR data, 3) destriping, 4) angular-shift correction, 5) noise reduction, 6) smile–frown detection, 7)
 103 radiometric calibration, and 8) atmospheric correction.

104 The hyperspectral dataset need to geo-referencing dataset to the pixels located in right position,
 105 therefore we used relative geo-referencing.

106 **4.2. Results**

107 After of applying preprocessing, the spectral unmixing was used for extraction of the mineral
 108 map. The spectral unmixing algorithm was applied on hyperspectral dataset to create the mineral
 109 map. The Hysime algorithm detected 11 endmember on the area. Then endmember extraction
 110 applied by Sisal and N-finder algorithms. Finally, the abundance maps were obtained. In order to
 111 determine the nature of each mineral ore exactly, we attributed the extracted spectral signatures to
 112 the spectral signatures that are in the spectral library. Finally, we compared the obtained maps to the

113 maps that are in the geological report of Geological Survey and Mineral Exploration of Iran (GSI) in
114 order to more validation. The all of endmembers assigned to mineral ores that are: malachite, azurite,
115 chalcantite, limonite and hematite.

116 The figure 5-a presents the result of obtained maps from abundance of mineral ores in the area.
117 The obtained result of abundance map of copper has presented in figure 5-b. The figure 5-c presents
118 result of iron oxide such as limonite and hematite prominently.

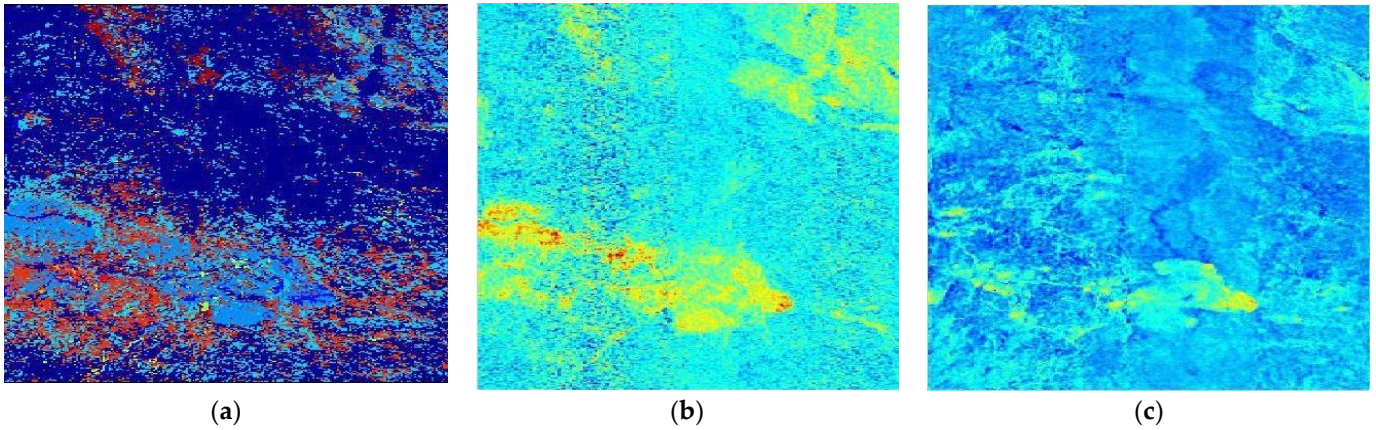


Figure 5. (a) The classification map of extracted spectral signatures, (b) The abundance map of copper oxide (malachite and azurite, prominently), and (c) The abundance map of iron oxide (limonite and hematite, prominently).

119 5. Conclusions

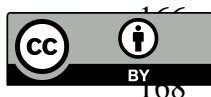
120 Remote sensing as a new technology can provide information about geology and mineral
121 exploration with lowest price at least time. In this case, hyperspectral images with having rich
122 spectral information are able to be effective for improvement in the results. Due to low spatial
123 resolution of hyperspectral images, we applied a new technique that is based on unmixing. This
124 technique has the ability to extract types of variety of mineral ores and alterations consequently. In
125 this study, we used hyperspectral data that obtained by Hyperion sensor in Meyduk area and
126 recognized some prominent mineral ores like malachite, azurite, chalcantite, limonite and hematite.
127 We presented the prominent abundance maps and recognized the nature of each mineral ore using
128 spectral signature. Finally, sericite and argillic alterations were detected that have good agreement
129 with the geological report.

130 **Acknowledgments:** We would like to thank Geological Survey and Mineral Exploration of Iran (GSI) for
131 providing the geological report of the area.

132 References

- 133 1. Seydi, S. T.; Hasanlou, M. A new land-cover match-based change detection for hyperspectral imagery. *Eur.*
134 *J. Remote Sens.* 2017, 50, 517–533.
- 135 2. Hussain, M.; Chen, D.; Cheng, A.; Wei, H.; Stanley, D. Change detection from remotely sensed images:
136 From pixel-based to object-based approaches. *ISPRS J. Photogramm. Remote Sens.* 2013, 80, 91–106,
137 doi:10.1016/j.isprsjprs.2013.03.006.
- 138 3. Seydi, S. T.; Hasanlou, M. Novel Wetland and Water Body Change Detction using Multitemporal
139 Hyperspectral Imagery. In; *Springer: Oman, Muscat*, 2016.
- 140 4. Melesse, A. M.; Weng, Q.; Thenkabail, P. S.; Senay, G. B. Remote sensing sensors and applications in
141 environmental resources mapping and modelling. *Sensors* 2007, 7, 3209–3241.
- 142 5. Carrino, T. A.; Crósta, A. P.; Toledo, C. L. B.; Silva, A. M. Hyperspectral remote sensing applied to mineral
143 exploration in southern Peru: A multiple data integration approach in the Chapi Chiara gold prospect. *Int.*
144 *J. Appl. Earth Obs. Geoinformation* 2017.

- 145 6. Crósta, A. P.; de Souza Filho, C. R. Hyperspectral remote sensing for mineral mapping: a case-study at alto
146 Paraíso de Goiás, central Brazil. *Rev. Bras. Geociências* 2017, 30, 551–554.
- 147 7. Roonwal, G. S. Remote Sensing in Mineral Exploration. In *Mineral Exploration: Practical Application*;
148 *Springer*, 2018; pp. 119–153.
- 149 8. Ertürk, A.; Güllü, M. K.; Çeşmeci, D.; Gerçek, D.; Ertürk, S. Spatial resolution enhancement of hyperspectral
150 images using unmixing and binary particle swarm optimization. *IEEE Geosci. Remote Sens. Lett.* 2014, 11,
151 2100–2104.
- 152 9. Xu, X.; Shi, Z. Multi-objective based spectral unmixing for hyperspectral images. *ISPRS J. Photogramm.*
153 *Remote Sens.* 2017, 124, 54–69.
- 154 10. Nascimento, J. M.; Bioucas-Dias, J. M. Hyperspectral signal subspace estimation. In *Geoscience and Remote*
155 *Sensing Symposium, 2007. IGARSS 2007. IEEE International; IEEE, 2007; pp. 3225–3228.*
- 156 11. Winter, M. E. N-FINDR: an algorithm for fast autonomous spectral end-member determination in
157 hyperspectral data. In *SPIE's International Symposium on Optical Science, Engineering, and Instrumentation*;
158 *International Society for Optics and Photonics*, 1999; pp. 266–275.
- 159 12. Heinz, D. C.; others Fully constrained least squares linear spectral mixture analysis method for material
160 quantification in hyperspectral imagery. *IEEE Trans. Geosci. Remote Sens.* 2001, 39, 529–545.
- 161 13. Boomeri, M.; Nakashima, K.; Lentz, D. R. The Miduk porphyry Cu deposit, Kerman, Iran: A geochemical
162 analysis of the potassic zone including halogen element systematics related to Cu mineralization processes.
163 *J. Geochem. Explor.* 2009, 103, 17–29.
- 164 14. Khurshid, K. S.; Staenz, K.; Sun, L.; Neville, R.; White, H. P.; Bannari, A.; Champagne, C. M.; Hitchcock, R.
165 Preprocessing of EO-1 Hyperion data. *Can. J. Remote Sens.* 2006, 32, 84–97.



© 2018 by the authors; licensee MDPI, Basel, Switzerland. This article is an open access article distributed under the terms and conditions of the Creative Commons Attribution (CC-BY) license (<http://creativecommons.org/licenses/by/4.0/>).